High resolution localized two-dimensional MR spectroscopy in mouse brain in vivo

Braakman, N.; Oerther, T.; Groot, H.J.M. de; Alia, A.

Magnetic Resonance in Medicine 60:449–456 (2008)

High Resolution Localized Two-Dimensional MR Spectroscopy in Mouse Brain In Vivo

Niels Braakman,[1] Thomas Oerther,[2] Huub J.M. de Groot,[1] and A. Alia[1*]

Localized two-dimensional MR spectroscopy (2D MRS) is impacting the in vivo studies of brain metabolites due to improved spectral resolution and unambiguous assignment opportunities. Despite the large number of transgenic mouse models available for neurological disorders, localized 2D MRS has not yet been implemented in the mouse brain due to size constraints. In this study we optimized a localized 2D proton chemical shift correlated spectroscopic sequence at field strength of 9.4T to obtain highly resolved 2D spectra from localized regions in mouse brains in vivo. The combination of the optimized 2D sequence, high field strength, strong gradient system, efficient water suppression, and the use of a short echo time allowed clear detection of cross-peaks of up to 16 brain metabolites, allowing their direct chemical shift assignments in vivo. To our knowledge this is the first in vivo 2D MRS study of the mouse brain, demonstrating its feasibility to resolve and simultaneously assign several metabolite resonances in the mouse brain in vivo. Implementation of 2D MRS will be invaluable in the identification of new biomarkers during disease progression and treatment using the various available mouse models. Magn Reson Med 60:449–456, 2008. © 2008 Wiley-Liss, Inc.

Key words: two dimensional MRS; L-COSY; mouse brain; resonance assignment

Proton MR spectroscopy (MRS) is an indispensable tool for noninvasive in vivo analysis of brain metabolites. MRS is increasingly used in the area of neurodegenerative diseases and other brain illnesses (1,2) especially due to the realization of its potential role in identifying crucial in vivo biomarkers of these diseases (3,4). However, low concentrations of several brain metabolites and difficulty in separating the resonances of metabolites with coupled spin systems restricts the application of in vivo 1D MRS in identifying potential biomarkers of these diseases. In contrast to localized 1D MRS, localized two-dimensional (2D) MRS overcomes the problem of spectral overlap considerably because the resonances are spread over a two-dimensional surface rather than along a single frequency dimension. In addition, 2D MRS provides spectral assignment opportunities stemming from correlations between pairs of related resonances. Thus in vivo application of localized 2D MRS can allow separation and unambiguous assignment of resonances of several metabolites in a single measurement (5). The linear relationship between cross-peak volume and concentration has been previously used for quantification of metabolites using 2D MRS (6–8). Several studies in humans (9–12) and a few studies in rats (6,7,13) have shown promising results with localized 2D MRS by correctly distinguishing metabolites that could not be unambiguously identified using 1D MRS. However, due to a low signal-to-noise ratio, a relatively low number of molecules could be clearly detected and a bigger sample volume (voxel) was necessary to achieve reasonable temporal resolution. Thus improvement in signal-to-noise ratio of in vivo localized 2D MRS is still necessary for exploiting its potential benefits in terms of resolution and assignment opportunities.

A large number of transgenic mouse models are currently available for various brain disorders, including neurodegenerative diseases (4). Due to sensitivity issues and its small size, 2D MRS has not yet been implemented in mouse brain (5). Successful implementation of 2D MRS in mice will greatly benefit studies of neurological diseases, by identifying crucial in vivo biomarkers in the various transgenic mouse models available for these diseases.

In this study, we implemented and optimized a PRESS-based localized 2D ^{1}H homonuclear correlation spectroscopy sequence on a 9.4T MRI scanner using a phantom solution and obtained for the first time highly resolved localized 2D MR spectra from the living mouse brain. In comparison to the earlier in vivo localized 2D studies in rat brain at 7T (7), we achieved significantly higher signal-to-noise ratio in a smaller voxel of only 27 μL and provide direct in vivo assignment of several brain metabolites in a single measurement in mouse brain.

MATERIALS AND METHODS

Mice

Six female C57bl6J mice aged between 5 and 6 months were used in this study. All animal experiments were approved by the Institutional Animal Care and Animal Use Committee in accordance with the NIH Guide for the care and Use of Laboratory Animals. For all in vivo MR measurements, the mice were anesthetized and their respiration rate and temperature was constantly monitored as described earlier (14).

Brain Phantom

As a reference for the in vivo measurements, a brain phantom was designed that contained 11 different brain metab-

[1]SSNMR, Leiden Institute of Chemistry, Gorlaeus Laboratoria, Leiden, The Netherlands.

[2]Bruker BioSpin GmbH, NMR Microscopy, Rheinstetten, Germany.

*Correspondence to: A. Alia, Leiden Institute of Chemistry, Gorlaeus Laboratoria, PO Box 9502, 2300 RA Leiden, The Netherlands. E-mail: a.alia@chem.leidenuniv.nl

Received 1 October 2007; revised 14 March 2008; accepted 21 March 2008.

DOI 10.1002/mrm.21662

Published online in Wiley InterScience (www.interscience.wiley.com).

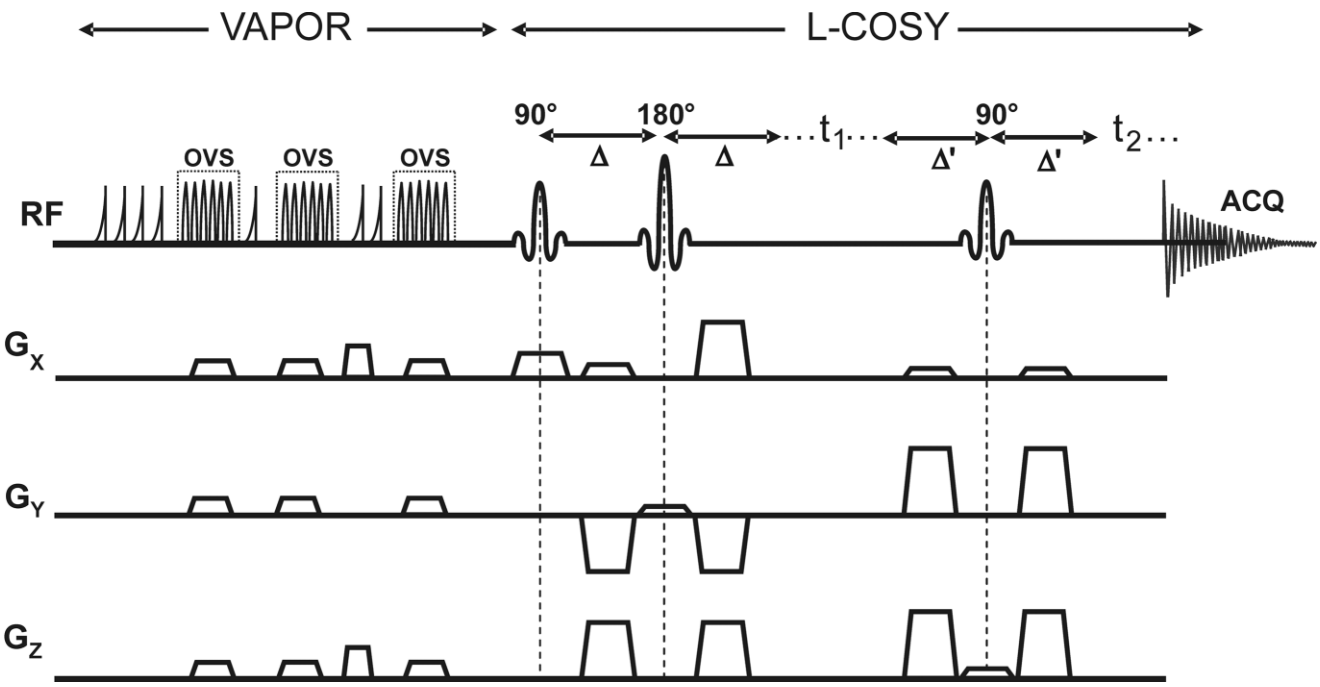

FIG. 1. The pulse sequence of 2D L-COSY preceded by a VAPOR sequence for global water suppression interleaved with outer volume suppression (OVS). The initial value of TE = 15 ms, consisting of two separate echo times; TE_1 (6 ms) and TE_2 (9 ms). The values of the variables in the figure are determined as follows: $\Delta = TE_1/2$; $t_1 = TE_1 + \Delta t_1$; $\Delta' = TE_2/2$.

olites in physiologically relevant concentrations. The phantom was made in potassium phosphate buffer (50 mM; pH 7.5) containing the following metabolites: creatine hydrate (10 mM), N-acetyl-DL-aspartic acid (12.5 mM), phosphocreatine sodium salt (4 mM), choline chloride (3 mM), L-glutamine (1.5 mM), L-glutamic acid (12.5 mM), glutathione (1.25 mM), gamma-aminobutyric acid (1.8 mM), myo-inositol (7.5 mM), taurine (1 mM), and DL-lactic acid (5 mM). The final pH of the brain phantom was 7.5. All chemicals were purchased from Sigma-Aldrich Chemie BV (Netherlands).

MR Spectroscopy

All measurements were conducted at 25° on a vertical wide-bore 9.4T Bruker Avance 400WB spectrometer, with a 1000 mTm^{-1} actively shielded imaging gradient insert (Bruker BioSpin). The radiofrequency (RF) coil used was a 25-mm volume coil, specifically, a birdcage transmit/receive coil (Bruker BioSpin). The system was interfaced to a Linux pc running Topspin 1.5 and Paravision 4.0 imaging software (Bruker BioSpin).

Localized T_2-weighted multislice rapid acquisition with relaxation enhancement (RARE) images were acquired to select a volume of interest (voxel) as described previously (14). The MRS voxels were localized either in (a) the middle of the mouse brain, covering predominantly the thalamus region and some parts of the hippocampus ($4 \times 4 \times 4$ mm^3; 64 μL), or (b) in the cortex–hippocampus regions in the mouse brain ($1.7 \times 4 \times 4$ mm^3; 27 μL). The local field homogeneity was optimized by adjustment of first- and second-order shim coil currents using the FASTMAP sequence. The field homogeneity in a 27–64 μL voxel typically resulted in water line-widths of 5–11 Hz in phantoms and ~16–20 Hz in live mouse brain.

The PRESS (Point Resolved Spectroscopy) sequence (15) was used for 1D localized ^1H MR spectroscopy. This sequence uses three hermite RF pulses (90°, 180°, 180°). The sequence details are described by Mandal (2). The repetition time (TR) and echo time (TE) were 1500 ms and 15 ms, respectively. The PRESS sequence used 2048 complex points, with a spectral width of 10 ppm. The final 1D spectra were obtained with number of scans = 512 and a scan times of approximately 13 min.

For 2D localized MRS, the PRESS protocol was modified based on the study of Thomas et al. (10) to generate a localized 2D chemical shift correlated spectroscopic sequence (L-COSY) for the 9.4T MR spectrometer. The resulting PRESS based L-COSY sequence was integrated in the Paravision 4.0 imaging software (Bruker BioSpin) and is shown in Figure 1. The sequence consists of three RF pulses (90°, 180°, 90°), slice-selective along three orthogonal axes. The last slice-selective 90° RF pulse also served as a coherence transfer pulse for the L-COSY spectrum necessary for correlating the metabolites peak in the second dimension. Optimized hermite 90° and 180° RF pulses with 1 ms durations were used for localization. The bandwidth of 90° and 180° RF pulses were 5.4 KHz and 3.4 KHz, respectively. A total of 16 phase cycles for all the three RF pulses were used for each localized Δt_1 increment. To achieve a short echo time of 15 ms, the duration of the spoiler gradient necessary to dephase the unwanted magnetization from outside the voxel was kept to a minimum. Both the 1D PRESS sequence and 2D L-COSY sequences were preceded by a VAPOR (Variable Pulse power

and Optimized Relaxation delays) sequence (16) for global water suppression. The sequence consists of 7 variable power RF pulses with an optimized relaxation delay. The relaxation delays t1–t7 between the consecutive pulses were 150, 80, 160, 80, 100, 37.11, and 57.36 ms, respectively. Water suppression bandwidth was set at 350 Hz. Outer volume suppression (OVS) was combined in an interleaved mode with the water suppression scheme, thus improving the localization performance and reducing the demands for spoiler gradients. The OVS scheme used a total of 18 "hyperbolic secant" RF pulses, each with 90° nominal flip angle and 1-ms pulse length. The OVS slice thickness was 4 mm with a 0-mm gap to the voxel.

Localized 2D MR spectra were recorded using a TE of 15 ms (TE_1 = 6 ms and TE_2 = 9 ms), and a TR of 1500 ms (Fig. 1). To obtain a feasible scan time 2D MR spectra were recorded using 2048 complex points along F2 and 192 points (incremental excitation steps) along F1, with a spectral width of 11 ppm and 20 averages per excitation step. This resulted in a total of 3840 scans (192 Δt_1 increments and 20 NEX/Δt_1), yielding a total scan time of approximately 1 hr 36 min. For the data in the F2 direction only the first 1024 data points were used. The data in the F1 direction was zero-filled to 1024 points, yielding a square matrix. Subsequently a squared sine windowing function was applied, with a sine bell shift of 8. Spectra were symmetrized to eliminate noise and obtain clearly defined cross-peaks. Processed data are presented in magnitude mode. The in vivo 2D spectra were referenced to the diagonal peak of Cr at 3.02 ppm.

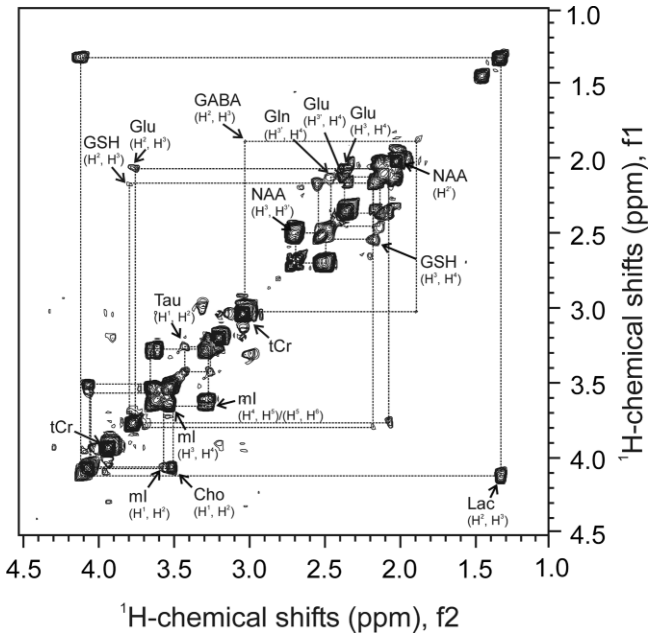

FIG. 2. High resolution localized 2D MR spectrum obtained from 64 μL voxel placed in a brain phantom composed of 11 brain metabolites, namely creatine (Cr), N-acetyl-DL-aspartic acid (NAA), phosphocreatine (PCr), choline (Cho), glutamine (Gln), glutamate (Glu), glutathione (GSH), gamma-aminobutyric acid (GABA), *Myo*-inositol (mI), taurine (Tau), and lactate (Lac). Spectra were obtained at 9.4 T using TR = 1500 ms and TE = 15 ms. The 2D data set was apodized with a QSINE function and zero filled to 1024 in both dimensions. A summary of the chemical shifts assignments and cross-peaks is presented in Table 1.

RESULTS AND DISCUSSION

In Vitro Study

Figure 2 shows a highly resolved 2D MR spectrum obtained from the 64 μL voxel placed at the center of the brain phantom. Despite low physiological concentrations of metabolites in the brain phantom and reasonably small voxel size of 64 μL, excellent spectral dispersion was achieved at 9.4 Tesla (T). In addition to the resonances of total creatine (tCr) that were assigned based on their diagonal peaks, 9 other metabolites can be directly assigned based on their network of cross-peaks in the 2D MR spectrum (Fig. 2). A summary of the assignment of metabolites is given in Table 1 (17). The cross-peak (H^2, H^3) of N-acetyl aspartate (NAA) is not visible in Figure 2. However, this cross-peak was present in the spectrum before symmetrization (data not shown) and was highly asymmetric, possibly due to the unequal effect of water suppression as also observed in previous 2D studies (6,12). As is clear from Figure 2 and Table 1, excellent separation of cross-peaks of the methylene protons of glutamate (Glu) (H^3–H^4; $H^{3'}$–H^4) and glutamine (Gln) ($H^{3'}$–H^4) is achieved using the 2D L-COSY sequence at 9.4 T from a small voxel of 64 μL. In addition, the cross-peaks of the Glu-moiety of glutathione (GSH) were clearly separated from free Glu (Fig. 2). The cross-peaks of choline (Cho) (H^1–H^2) and *myo*-Inositol (mI; H^1–H^2), which were overlapping at 3T in a previous phantom study (12) were clearly resolved in the present study (Fig. 2).

In Vivo Study

In vivo high resolution localized 2D MRS was performed in the mouse brain after image guided positioning of a 64 μL voxel (4 × 4 × 4 mm^3) in the center of the brain, covering predominantly the thalamus region and some parts of the hippocampus, as depicted in Figure 3a. A characteristic in vivo 1D MR spectrum of mouse brain from the same voxel is shown on top of the 2D MR spectrum in Figure 3b. Generally short echo time localization methods minimize T_2 relaxation effects, which increases the sensitivity and reliability of metabolite quantification (18). A short echo time of 15 ms was used for in vivo 2D MRS in the present study. As can be seen in Figure 3b, in vivo localized 2D MRS allowed separation of most overlapping peaks for the coupled spin systems that gave rise to off-diagonal peaks. The singlet resonance of the methyl group of NAA (2.0 ppm) appeared on the diagonal and protons from the aspartate moiety of NAA give rise to an off-diagonal peak, not contaminated by other resonances (Fig. 3b; Table 1). In addition, 2D spectra showed clear separation of the cross-peaks of Glu, Gln, GSH, and GABA, thus allowing the direct in vivo assignment of resonances of these coupled spin systems. A cross-peak at 2.35 ppm/1.95 ppm was assigned to the GABA moiety of homocarnosine (HCar), a dipeptide that consists of histidine and GABA (Fig. 3b). The resonances that overlap at 3.2 ppm in the 1D spectrum are resolved into cross-peaks of mI (H^5/H^4), taurine (Tau) (H^2/H^1), and phosphorylethanolamine

Table 1
Proton Chemical Shifts of Metabolites Obtained In Vivo (in the Mouse Brain) or In Vitro (Brain Phantom) From Localized 2D MR Spectra at 9.4T

Metabolites		Group		^{1}H-Chemical shift (ppm)*			Origin of cross-peaks
				In vitro		*In vivo*[φ]	
				In H_2O[ψ]	In phantom[φ]		
Ala		$^2CH_2$	(H^2)	3.77		3.8[a]	H^2-H^3
		$^3CH_3$	(H^3)	1.46		1.5[a]	
Asp		^2CH	(H^2)	3.89		3.9 [b]	H^2-H^3
		$^3CH_2$	($H^{3'}$)	2.80		2.89[b]	
Cho		$^1CH_2$	(H^1)	4.05	4.05		H^1-H^2
		$^2CH_2$	(H^2)	3.50	3.50		
Glc		^3CH	(H^3)	3.70		3.62[a]	H^3-H^4
							H^4-H^5
		^4CH	(H^4)	3.40		3.4[b]	
		^5CH	(H^5)	3.82		3.80[a,b]	
GABA		$^2CH_2$	(H^2)	3.01	3.02	3.0[a]	H^2-H^3
		$^3CH_2$	(H^3)	1.89	1.9	1.9[a], 1.86[b]	H^3-H^4
		$^4CH_2$	(H^4)	2.28		2.29[a], 2.2[b]	
Gln		^2CH	(H^2)	3.75		3.8[a]	H^2-H^3
		$^3CH_2$	($H^{3'}$)	2.13	2.13	2.17[a], 2.19[b]	H^3-H^4
		$^4CH_2$	(H^4)	2.45	2.46	2.49[a,b]	
Glu		^2CH	(H^2)	3.74	3.76	3.76[a], 3.78[b]	H^2-H^3
		$^3CH_2$	(H^3)	2.12	2.04	2.10[a]	H^3-H^4
			($H^{3'}$)	2.04	2.12	2.12[a], 2.17[b]	$H^{3'}$-H^4
		$^4CH_2$	(H^4)	2.34	2.38	2.47[a], 2.45[b]	
GPC		$^1CH_2$	(H^1)	3.61		3.72[a,b]	H^1-H^2
		^2CH	(H^2)	3.90		3.91[a,b]	
Gro		$^1CH_2$	(H^1)	3.55		3.52[b]	H^1-$H^{1'}$
							H^3-$H^{3'}$
			($H^{1'}$)	3.64		3.67[b]	
		$^3CH_2$	(H^3)	3.55		3.52[b]	
			($H^{3'}$)	3.64		3.67[b]	
GSH	Glutamate moiety	^2CH	(H^2)	3.77	3.78		H^2-H^3
		$^3CH_2$	(H^3)	2.16	2.18	2.17[a,b]	H^3-H^4
		$^4CH_2$	(H^4)	2.56	2.55	2.55[a,b]	
HCar	GABA moiety	$^3CH_2$	(H^3)	1.89		1.95[a]	H^3-H^4
		$^4CH_2$	(H^4)	2.37		2.35[a]	
Lac		^2CH	(H^2)	4.10	4.11	4.14[b]	H^2-H^3
		$^3CH_3$	(H^3)	1.31	1.31	1.33[b]	
mI		^1CH	(H^1)	3.52	3.56		H^1-H^2
		^2CH	(H^2)	4.05	4.05		H^2-H^3
		^3CH	(H^3)	3.52	3.56		H^3-H^4
		^4CH	(H^4)	3.61	3.67	3.62[a,b]	H^4-H^5
		^5CH	(H^5)	3.27	3.27	3.29[a], 3.25[b]	H^5-H^6
		^6CH	(H^6)	3.61	3.67	3.62[a,b]	
NAA	Acetyl moiety	$^{2'}CH_3$	($H^{2'}$)	2.01	2.04	2.02[a,b]	H^3-$H^{3'}$
	Aspartate moiety						
		$^3CH_2$	(H^3)	2.67	2.67	2.70[a,b]	
			($H^{3'}$)	2.49	2.5	2.50[a,b]	
NAAG	Aspartate moiety	$^3CH_2$	(H^3)	2.72		2.78[a], 2.74[b]	H^3-$H^{3'}$
			($H^{3'}$)	2.52		2.55[a], 2.51[b]	
PEA		$^1CH_2{}^2CH_2$	(H^1)	3.98		3.98[a]	H^1-H^2
			(H^2)	3.22		3.27[a]	
Tau		$^1CH_2$	(H^1)	3.42	3.42	3.42[a,b]	H^1-H^2
		$^2CH_2$	(H^2)	3.25	3.26	3.25[a,b]	
Thr		^2CH	(H^2)	3.58		3.52[b]	H^2-H^3
		^3CH	(H^3)	4.25		4.2[b]	
Tyr		$^\alpha CH$	(H^α)	3.93		3.88[b]	H^α-H^β
		$^\beta CH_2$	(H^β)	3.19		3.1[b]	H^α-$H^{\beta'}$
		$^{\beta'}CH_2$	($H^{\beta'}$)	3.04		3.0[b]	

[ψ]Govindaraju et al. (17); [φ]This work; *Estimated accuracy ± 0.05 ppm.
[a]proton resonances seen *in vivo* in 64 μL voxel covering predominantly the thalamus region
[b]proton resonances seen *in vivo* in 27 μL voxel placed in cortex/hippocampus region.

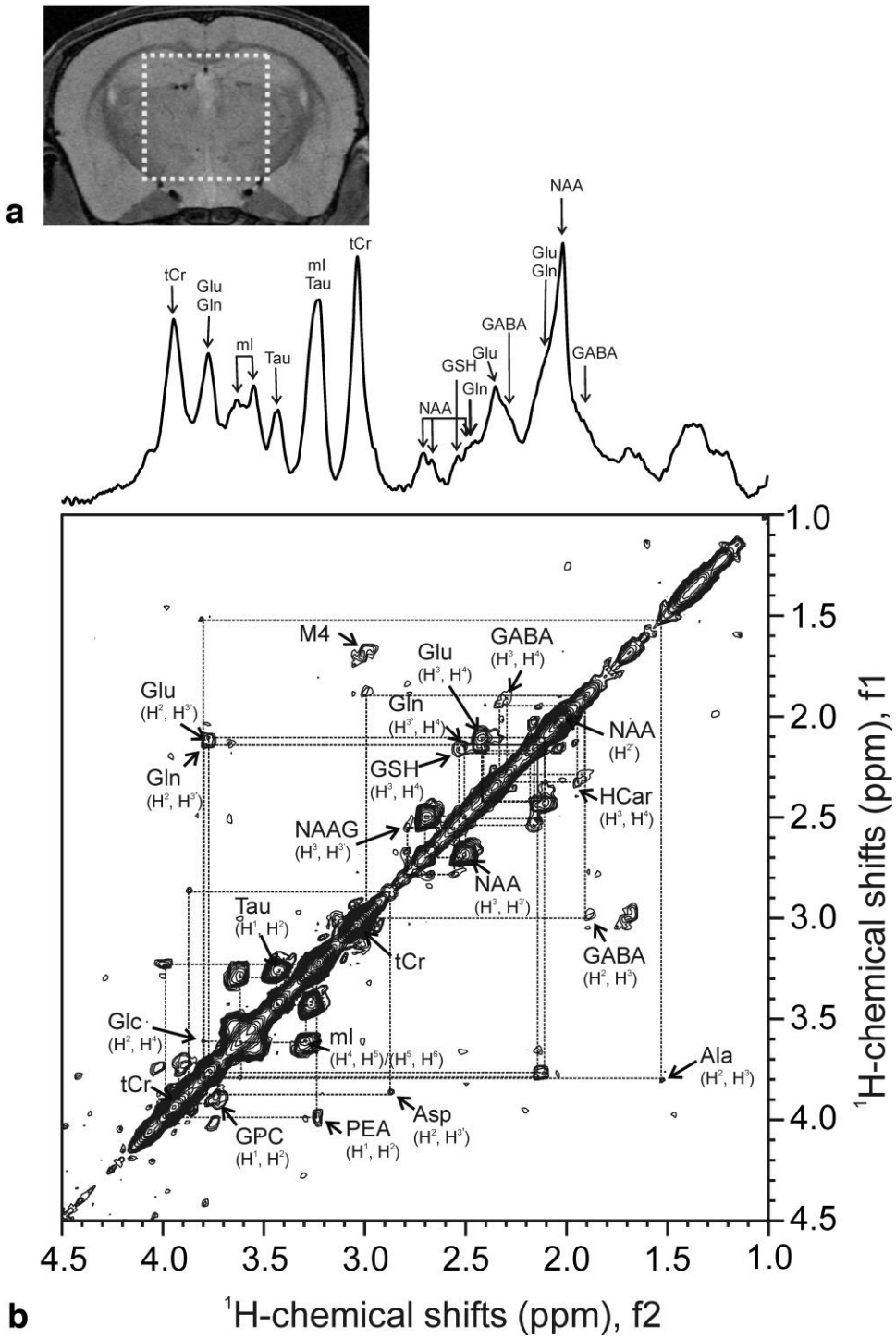

FIG. 3. In vivo high resolution localized 2D MR spectrum from mouse brain obtained at 9.4T. **a:** Coronal MR image of the mouse brain obtained by RARE sequence showing the position of the selected voxel of 64 μL (4 × 4 × 4 mm³) covering predominantly the thalamus region and some parts of hippocampus. **b:** The 2D MR spectrum from the selected 64 μL voxel in the mouse brain obtained by the PRESS based 2D L-COSY sequence as shown in Figure 1. A one dimensional spectrum from the same brain region (64 μL voxel) is shown on top of the 2D spectrum. Spectra were obtained using TR = 1500 ms and TE = 15 ms. The 2D data set was apodized with a QSINE function and zero filled to 1024 in both dimensions. A summary of the chemical shifts assignments and cross-peaks is presented in Table 1. The peak M4 arises from macromolecules and is labeled in accordance with Behar and Ogino (21). [Color figure can be viewed in the online issue, which is available at www.interscience.wiley.com.]

(PEA) (H^2/H^1), which could be clearly seen in the 2D spectrum (Fig. 3b). Comparison of the intensities of cross-peaks of Tau and mI reflects that the level of Tau was slightly higher than mI in the mouse brain. This is in contrast to human brain which contains four- to fivefold higher concentrations of mI than Tau (17,19). The higher

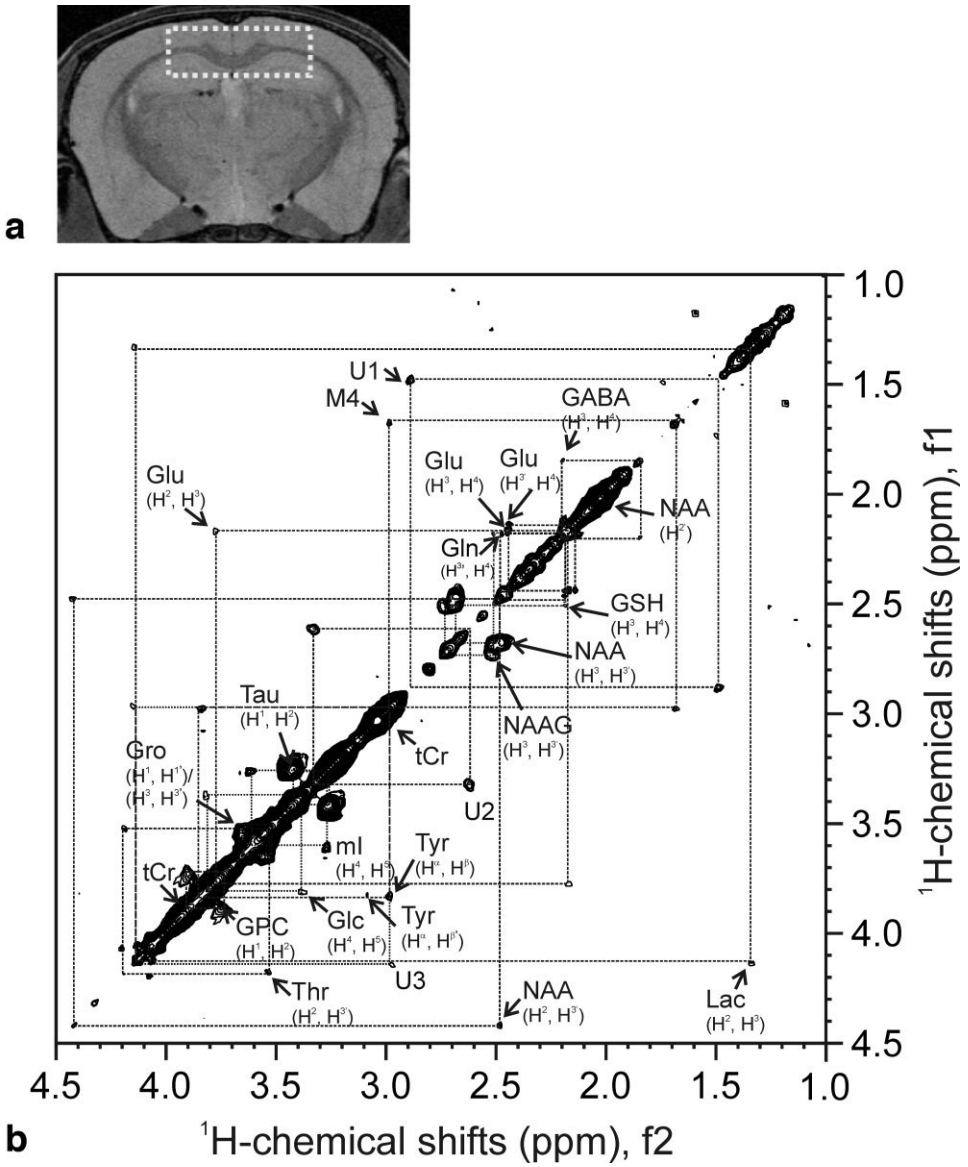

FIG. 4. In vivo high resolution localized 2D MR spectrum from the cortex–hippocampus region of the mouse brain obtained at 9.4T. **a:** Coronal MR image of the mouse brain obtained by RARE sequence showing the position of the selected voxel of 27 μL (1.7 × 4 × 4 mm^3) covering the cortex–hippocampus region. **b:** Two dimensional MR spectrum from the selected 27 μL voxel in the cortex–hippocampus region of the mouse brain obtained by the PRESS based 2D L-COSY sequence as shown in Figure 1. Spectra were obtained using TR = 1500 ms and TE = 15 ms. The 2D data set was apodized with a QSINE function and zero filled to 1024 in both dimensions. A summary of the chemical shifts assignments and cross-peaks is presented in Table 1. U1, U2, and U3 are unassigned cross-peaks. The peak M4 arises from macromolecules and is labeled in accordance with Behar and Ogino (21). Color figure can be viewed in the online issue, which is available at www.interscience.wiley.com.

level of Tau in comparison to mI in mice is consistent with levels reported by Tkac et al. (20) based on their 1D MRS data at 9.4T. The brain phantom used in this study contained 1 mM Tau, which is a physiologically relevant concentration for human brain. However, for a future mouse brain phantom, a concentration of up to 10 mM will be more relevant (20). The 2D spectrum in Figure 3b also shows well-resolved cross-peaks of many other metabolites present in lower concentrations, such as alanine (Ala), aspartate (Asp), and α-glucose (Glc). As can be seen in Figures 3b and 4b, only the α-anomer of glucose showed cross-peaks in the 2D spectra, despite the fact that the overall concentration of the β-anomer of glucose (β-Glc) is believed to be higher in brain than that of the α-anomer (α-Glc). Presently, we are unable to explain why the β-glucose did not show any cross-peak. However, our results are similar to earlier in vivo 2D MRS studies in human (12) and rat (8) brain where cross-peaks of only α-glucose were detected.

A complete map of the in vivo resonances of the observed cross-peaks is depicted in Table 1. A strong cross-peak at 3.0 ppm/1.7 ppm is assigned to macromolecules (M4) according to Behar and Ogino (21). It has been shown earlier that the contribution of macromolecule resonances

increases rapidly with decreasing echo time (16). Stronger signals from macromolecules in Figure 3b might have been due to the use of a short echo time of 15 ms in the present studies.

While a large voxel as shown in Figure 3b gave better signal-to-noise ratio in 2D spectra, a small voxel would be necessary to achieve regional specificity in the mouse brain. Especially localized information from regions such as the cortex and hippocampus which are more severely affected during neurodegenerative diseases would be invaluable. Figure 4b shows an in vivo 2D MR spectrum obtained from a smaller voxel ($1.7 \times 4 \times 4$ mm^3; 27 μL) that was positioned in the cortex and hippocampus region as shown in Figure 4a. Despite the small size of the voxel, the signal-to-noise ratio was sufficient to allow separation of most overlapping peaks, which resulted in clear identification and assignment of 15 brain metabolites. This was possible due to excellent localization performance, successful first and higher order shimming, efficient water suppression and careful optimization of acquisition parameters at high magnetic field (9.4T). Cross-peaks of Glu, Gln, and GSH were clearly separated. In addition, the cross-peak of NAAG was separated from NAA (Fig. 4b). NAAG is the most abundant peptide neurotransmitter in the human brain (17), and consists of NAA with a peptide bond to Glu. It is difficult to differentiate NAAG from NAA and Glu by in vivo 1D MRS. Recently Edden et al. (22), have used the MEGA-PRESS sequence to selectively separate the aspartyl spin system of NAA and NAAG. However, due to a low signal-to-noise ratio, a large voxel was necessary to observe the signal from NAAG. Moreover, only one spin system could be monitored at a time. As shown in Figure 4b, using 2D MRS at high magnetic field, we could separate the cross-peaks between aspartyl β-protons of NAA (2.70, 2.50 ppm) and NAAG (2.74, 2.51 ppm) in the same spectrum from the living mouse brain and could simultaneously detect many other metabolites in a single data set. Well resolved cross-peaks from mI and Tau were also detected. Of interest, the Tau/mI ratio is even higher in the cortex–hippocampus region (Fig. 4b) than in the center of the brain covering predominantly the thalamus region (Fig. 3b). This is evident from the intensities of the cross-peaks of these two metabolites in the cortex–hippocampus, suggesting that the cortex and hippocampus of the mouse brain contain very high concentrations of Tau in comparison to mI. The 2D MR spectrum also shows cross-peaks of α-glucose (Glc), tyrosine (Tyr), threonine (Thr), and Glycerol (Gro; Fig. 4b). Similar to previous studies (6,12), not all cross-peaks of these metabolites could be easily detected. Three cross-peaks labeled as U1, U2, and U3 were also observed (Fig. 4b) which could not be assigned to any of the 35 known brain metabolites (17). Further studies would be needed to assign these resonances to new metabolites or macromolecules present in the cortex–hippocampus region of the mouse brain. The in vivo resonance assignment of metabolites in the cortex–hippocampus region of mouse brain is summarized in Table 1.

In general, in comparison to 2D MRS, 1D MRS is a more efficient method for absolute quantification of metabolites when it is combined with data analysis methods such as LCmodel. For example, 16 brain metabolites were quantified in mouse brain using this method (20). Two dimensional MRS, however, allows unambiguous visualization of cross-peaks and thus has great potential to unearth unknown brain metabolites so far hidden under overlapping multiplets (7), which will have significant implication in detecting new biomarkers of various brain diseases in future.

In conclusion, the results presented in this study clearly demonstrate the feasibility of 2D MRS in combination with high magnetic field (9.4T) to get localized access to the mouse brain for efficient identification of metabolites. A large number of metabolites were assigned simultaneously without contamination based on their network of cross-peaks in localized regions of the mouse brain in vivo. These results suggest that localized 2D ^{1}H MRS at high field strength can offer greater scope for identifying potential biomarkers of neurological diseases using variety of transgenic mouse models.

ACKNOWLEDGMENTS

The authors thank Kees Erkelens and Fons Lefeber for their assistance during various stages of MRS measurements. This research project was supported in part by funds from Internationale Stichting Alzheimer Onderzoek (ISAO), CYTTRON within the Bsik program (Besluit subsidies investeringen kennisinfrastructuur) and the Centre for Medical Systems Biology (CMSB).

REFERENCES

1. Kantarci K, Petersen RC, Boeve BF, Knopman DS, Tang-Wai DF, O'Brien PC, Weigand SD, Edland SD, Smith GE, Ivnik RJ, Ferman TJ, Tangalos EG, Jack CR. 1H MR spectroscopy in common dementias. Neurology 2004;63:1393–1398.
2. Mandal PK. Magnetic resonance spectroscopy (MRS) and its application in Alzheimer's disease. Conc Magn Reson A 2007;30A:40–64.
3. Marjanska M, Curran GL, Wengenack TM, Henry PG, Bliss RL, Poduslo JF, Jack CR Jr, Ugurbil K, Garwood M. Monitoring disease progression in transgenic mouse models of Alzheimer's disease with proton magnetic resonance spectroscopy. Proc Natl Acad Sci U S A 2005;102:11906–11910.
4. Choi J-K, Dedeoglu A, Jenkins BG. Application of MRS to mouse models of neurodegenerative illness. NMR Biomed 2007;20:216–237.
5. Meric P, Autret G, Doan BT, Gillet B, Sebrie C, Beloeil JC. In vivo 2D magnetic resonance spectroscopy of small animals. MAGMA 2004;17:317–338.
6. Delmas F, Beloeil JC, van der Sanden BPJ, Nicolay K, Gillet B. Two-voxel localization sequence for in vivo two-dimensional homonuclear correlation spectroscopy. J Magn Reson 2001;149:119–125.
7. Welch JWR, Bhakoo K, Dixon RM, Styles P, Sibson NR, Blamire AM. In vivo monitoring of rat brain metabolites during vigabatrin treatment using localized 2D-COSY. NMR Biomed 2003;16:47–54.
8. Peres M, Fedeli O, Barrere B, Gillet B, Berenger G, Seylaz J, Beloeil J-C. In vivo identification and monitoring of changes in rat brain glucose by two-dimensional shift correlated NMR spectroscopy. Magn Reson Med 1992;27:356–361.
9. Thomas MA, Ryner LN, Mehta MP, Turski PA, Sorenson JA. Localized 2D J-resolved 1H MR spectroscopy of human brain. J Magn Reson Imaging 1996;6:453–459.
10. Thomas MA, Yue K, Binesh N, Davanzo P, Kumar A, Siegel B, Frye M, Curran J, Lufkin R, Martin P, Guze B. Localized two-dimensional shift correlated MR spectroscopy of human brain. Magn Reson Med 2001;46:58–67.

11. Ziegler A, Gillet B, Beloeil J, Macher J, Decorps M, Nedelec J. Localized 2D correlation spectroscopy in human brain at 3T. MAGMA 2001;14: 45–49.
12. Thomas MA, Hattori N, Umeda M, Sawada T, Naruse S. Evaluation of two-dimensional L-COSY and PRESS using a 3 T MRI scanner: from phantoms to human brain in vivo. NMR Biomed 2003;16:245–251.
13. Von Kienlin M, Ziegler A, Le Fur Y, Rubin C, Decorps M, Remy C. 2D-spatial/2D-spectral spectroscopic imaging of intracerebral gliomas in rat brain. Magn Reson Med 2000;43:211–219.
14. Braakman N, Matysik J, van Duinen SG, Verbeek F, Schliebs R, de Groot HJM, Alia A. Longitudinal assessment of Alzheimer's beta-amyloid plaque development in transgenic mice monitored by in vivo magnetic resonance microimaging. J Magn Reson Imaging 2006; 24:530–536.
15. Bottomley PA. Spatial localization in NMR spectroscopy in vivo. Ann N Y Acad Sci 1987;508:333–348.
16. Tkac I, Starcuk Z, Choi IY, Gruetter R. In vivo 1H NMR spectroscopy of rat brain at 1 ms echo time. Magn Reson Med 1999;41:649–656.
17. Govindaraju V, Young K, Maudsley AA. Proton NMR chemical shifts and coupling constants for brain metabolites. NMR Biomed 2000;13: 129–153.
18. Pfeuffer J, Tkac I, Provencher SW, Gruetter R. Toward an in vivo neurochemical profile: quantification of 18 metabolites in short echo-time 1H NMR spectra of the rat brain. J Magn Reson 1999;141: 104–120.
19. van Zijl PCM, Barker PB. Magnetic resonance spectroscopy and spectroscopic imaging for the study of brain metabolism. Ann N Y Acad Sci 1997;820:75–96.
20. Tkac I, Henry PG, Andersen P, Keene CD, Low WC, Gruetter R. Highly resolved in vivo 1H NMR spectroscopy of the mouse brain at 9.4 T. Magn Reson Med 2004;52:478–484.
21. Behar KL, Ogino T. Characterization of macromolecule resonances in the 1H-NMR spectrum of rat brain. Magn Reson Med 1993;30:38–44.
22. Edden RA, Pomper MG, Barker PB. In vivo differentiation of N-acetyl aspartyl glutamate from N-acetyl aspartate at 3 Tesla. Magn Reson Med 2007;57:977–982.

WOULD YOU LIKE TO POST AN INFORMAL COMMENT ABOUT THIS PAPER, OR ASK THE AUTHORS A QUESTION ABOUT IT?

If so, please visit https://mrm.ismrm.org/ and register for our Magn Reson Med Discourse site (registration is free).

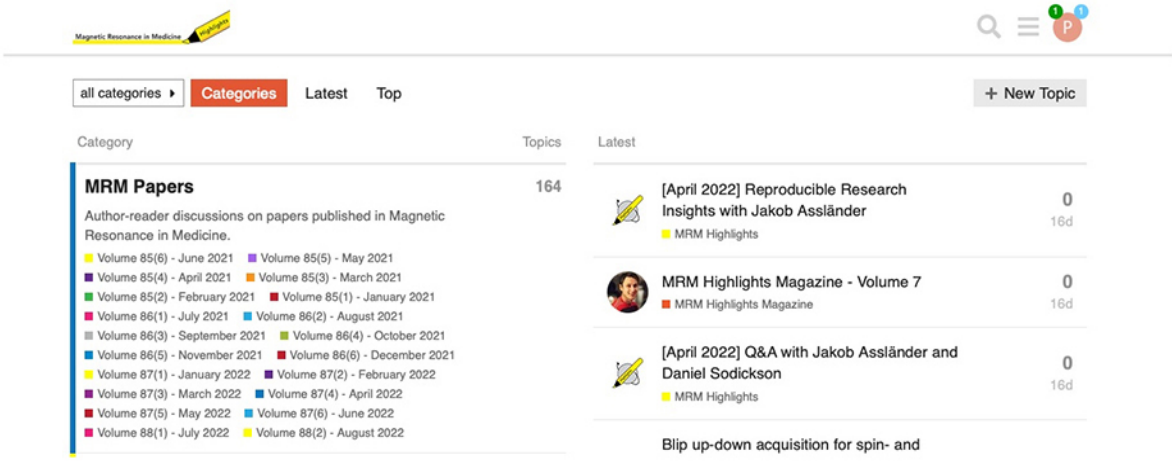

Magn Reson Med is currently listing the top 8 downloaded papers from each issue (including Editor's Picks) for comments and questions on the Discourse web site.

However, we are happy to list this or any other papers (please email mrm@ismrm.org to request the posting of any other papers.)

We encourage informal comment and discussion about Magn Reson Med papers on this site. Please note, however, that a formal errata from the authors should still be submitted in the usual way via our Manuscript Central online submission system.